










RESEARCH ARTICLE

Development of a dual antigen lateral flow immunoassay for detecting *Yersinia pestis*

Derrick Hau , Brian Wade , Chris Lovejoy , Sujata G. Pandit, Dana E. Reed, Haley L. DeMers, Heather R. Green , Emily E. Hannah , Megan E. McLarty, Cameron J. Creek , Chonnikarn Chokapirat, Jose Arias-Umana , Garrett F. Cecchini, Teerapat Nualnoi , Marcellene A. Gates-Hollingsworth, Peter N. Thorkildson, Kathryn J. Pflughoeft, David P. AuCoin *

Department of Microbiology and Immunology, University of Nevada, Reno School of Medicine, Reno, Nevada, United States of America

* daucoin@med.unr.edu



Abstract

Background

Yersinia pestis is the causative agent of plague, a zoonosis associated with small mammals. Plague is a severe disease, especially in the pneumonic and septicemic forms, where fatality rates approach 100% if left untreated. The bacterium is primarily transmitted via flea bite or through direct contact with an infected host. The 2017 plague outbreak in Madagascar resulted in more than 2,400 cases and was highlighted by an increased number of pneumonic infections. Standard diagnostics for plague include laboratory-based assays such as bacterial culture and serology, which are inadequate for administering immediate patient care for pneumonic and septicemic plague.

Principal findings

The goal of this study was to develop a sensitive rapid plague prototype that can detect all virulent strains of *Y. pestis*. Monoclonal antibodies (mAbs) were produced against two *Y. pestis* antigens, low-calcium response V (LcrV) and capsular fraction-1 (F1), and prototype lateral flow immunoassays (LFI) and enzyme-linked immunosorbent assays (ELISA) were constructed. The LFIs developed for the detection of LcrV and F1 had limits of detection (LOD) of roughly 1–2 ng/mL in surrogate clinical samples (antigens spiked into normal human sera). The optimized antigen-capture ELISAs produced LODs of 74 pg/mL for LcrV and 61 pg/mL for F1 when these antigens were spiked into buffer. A dual antigen LFI prototype comprised of two test lines was evaluated for the detection of both antigens in *Y. pestis* lysates. The dual format was also evaluated for specificity using a small panel of clinical near-neighbors and other Tier 1 bacterial Select Agents.

Conclusions

LcrV is expressed by all virulent *Y. pestis* strains, but homologs produced by other *Yersinia* species can confound assay specificity. F1 is specific to *Y. pestis* but is not expressed by all

OPEN ACCESS

Citation: Hau D, Wade B, Lovejoy C, Pandit SG, Reed DE, DeMers HL, et al. (2022) Development of a dual antigen lateral flow immunoassay for detecting *Yersinia pestis*. PLoS Negl Trop Dis 16(3): e0010287. <https://doi.org/10.1371/journal.pntd.0010287>

Editor: Anne-Sophie Le Guern, Institut Pasteur, FRANCE

Received: September 10, 2021

Accepted: February 28, 2022

Published: March 23, 2022

Peer Review History: PLOS recognizes the benefits of transparency in the peer review process; therefore, we enable the publication of all of the content of peer review and author responses alongside final, published articles. The editorial history of this article is available here: <https://doi.org/10.1371/journal.pntd.0010287>

Copyright: © 2022 Hau et al. This is an open access article distributed under the terms of the [Creative Commons Attribution License](https://creativecommons.org/licenses/by/4.0/), which permits unrestricted use, distribution, and reproduction in any medium, provided the original author and source are credited.

Data Availability Statement: All relevant data are within the manuscript and its [Supporting Information](#) files.

Funding: Funding from the Naval Research Laboratory contract ND0173-16-C-2003 (DA) supported the generation of mAbs and ELISA development. Funds from a Defense Threat Reduction Agency (DTRA) contract HDTRA1-16-C-0026 (DA) expanded the library of mAbs and allowed for the development and optimization of LFIs. The funders had no role in study design, data collection and analysis, decision to publish, or preparation of the manuscript.

Competing interests: I have read the journal's policy and the authors of this manuscript have the following competing interests: The goal of this research funded by Naval Research Laboratory contract ND0173-16-C-2003 and the Defense Threat Reduction Agency (DTRA) contract HDTRA1-16-C-0026 was to develop a diagnostic for plague. Currently the project is funded to transition these prototypes into an FDA approved diagnostic for plague through the MCDC contract # MCDC OTA W15QKN-16-9-1002.

virulent strains. Utilizing highly reactive mAbs, a dual-antigen detection (multiplexed) LFI was developed to capitalize on the diagnostic strengths of each target.

Author summary

Immunoassays were developed for the detection of two *Y. pestis* proteins, LcrV and F1, which have been characterized as potential biomarkers of plague. A total of twenty-two high affinity mAbs were isolated from BALB/c mice immunized with recombinant LcrV, F1 and F1-LcrV fusion protein via hybridoma technology. MAbs were characterized by Western blots, ELISA, and surface plasmon resonance. Antigen-capture LFIs and ELISAs were developed using the mAbs and optimized for analytical sensitivity. Prototype LFIs were evaluated to detect LcrV and F1 in surrogate clinical samples. A multiplexed LFI detecting both LcrV and F1 was assessed against a panel of *Y. pestis* isolates, clinically relevant near neighbors, and other bacterial Select Agents indicating high assay specificity. The prototype immunoassays will now need to be validated with multiple clinical matrices (i.e., whole blood), patient samples, and a larger specificity panel.

Background

Plague is a febrile illness caused by *Yersinia pestis*, a Gram-negative, nonmotile coccobacillus. The bacterium was responsible for the Black Death, which devastated over a third of Europe's population between 1347–1353 [1]. The Centers for Disease Control and Prevention classifies *Y. pestis* as a Tier 1 Select Agent due to its infectious nature, high mortality rates, threat to public health, and potential as a biothreat. The spread of *Y. pestis* is facilitated by small mammals and insect vectors. The bacterium is transmitted to humans through flea bites, contact with animal excretions, or inhalation of aerosolized droplets. The different routes of infection lead to three forms of plague: bubonic, pneumonic, and septicemic. Bubonic plague is easily diagnosed by the inflammation of lymph nodes resulting in the formation of painful swellings called buboes. Bubonic plague is the least fatal of the three forms, with a 40–70% case fatality rate (CFR) when left untreated; however, bubonic plague may develop into more serious forms of the infection [2]. Pneumonic and septicemic plague present with nonspecific flu-like symptoms, leading to death in as few as three days post-exposure [3]. The CFR for pneumonic and septicemic infections approach 100% when left untreated [2]. Time is a critical factor for treating plague as effective therapeutics must be administered within 20 hours from the onset of symptoms to ensure the best chance for patient survival [4].

Y. pestis is a zoonotic bacterium found in all geographical regions besides Oceania, with Madagascar and the Democratic Republic of Congo being primary hot spots for annual plague outbreaks [5,6]. Madagascar had accounted for 74% of all cases reported to the World Health Organization between 2010 and 2015 [7]. During this period, 200–700 cases were reported annually, mainly in the form of bubonic plague which is rarely transmissible human-to-human [8,9]. During the 2017 plague season, Madagascar reported a total of 2,417 cases of plague with a CFR of 8.6% [10]. Identification of the initial cluster of infections allowed for a proper response to prevent a larger epidemic [11]. This outbreak not only marked an increase in overall cases, but more importantly, an increased percentage of pneumonic infections (70% of total infections) [8,11]. The increase in pneumonic infections may, in part, be attributed to human-to-human transmission that occurred via infectious droplets [12–14]. This along with

high mortality rates of pneumonic infections warrant the need for development of additional countermeasures for plague.

The gold standard for diagnosing plague is bacterial culture [15]. Patient serology can be used to indicate if an individual was infected with *Y. pestis*; however, this method is hindered by its capacity to detect active infections as an antibody response is delayed upon exposure and a positive result may be due to a previous exposure [15–17]. These methods can be time consuming and require specialized laboratories and trained technicians. Advancements in rapid diagnostic tests (RDT) such as LFIs have made the detection of *Y. pestis* more feasible in low-technology settings and are instrumental in controlling plague outbreaks in endemic regions. A comparative study on various diagnostic methods has deemed an LFI to be an ideal platform for diagnosing plague [18]. LFIs are rapid, membrane-based immunoassays using antibodies linked to gold-nanoparticles for visual detection. Temperature stable reagents and user-friendly protocols make LFIs ideal for resource limited settings. The current LFI used in Madagascar detects the F1 antigen and has a sensitivity range of 25–100% and a specificity range of 59–79% when compared to bacterial culture and PCR [19–23]. Of concern, however, is that F1⁻ strains, mutants that do not express the F1 pilus structure, have been identified in clinical as well as laboratory settings [19,24,25]. In the present study, we describe the initial evaluation of a prototype multiplexed RDT that allows for detection of two *Y. pestis* antigens.

Y. pestis is a facultative anaerobe equipped with several virulence factors to allow survival within macrophages and in extracellular spaces [26]. Genes encoding virulence factors are dispersed throughout the genome, and are also encoded on three plasmids (pCD1, pPCP1, pMT1) [27]. Current LFIs used to diagnose plague detect F1, a protein encoded by the *cafI* gene on pMT1, a plasmid unique to *Y. pestis* [18,25,28]. The 15.5 kDa F1 antigen polymerizes to form a filament capsule surrounding the bacterium, protecting it from phagocytosis [29]. Expression of F1 is temperature-induced at >33°C [28]. The antigen is known to be shed during infection, making it a viable candidate biomarker for diagnosing plague [30–32]. Though attenuated in its ability to cause bubonic plague, F1⁻ isolates remain highly virulent by the inhalation route leading to pneumonic infections [25,33].

The pCD1 plasmid carries genes encoding a type-III secretion system (T3SS) and its related effector proteins [34]. The pCD1 plasmid is found in clinically relevant neighbors *Y. pseudotuberculosis* and *Y. enterocolitica* [35]. The T3SS is associated with a low-calcium response crucial for pathogenicity of *Yersinia* species [34]. Low-calcium response V (LcrV) is a multifunctional protein serving as the needle tip of the T3SS to translocate *Yersinia* outer proteins into host cells [36]. LcrV is also translocated during the process and suppresses the host inflammatory response by upregulating interleukin 10 via Toll-like receptor 2 [37]. Mutations in *lcrV* lead to avirulence in mice due to the inability to translocate effector proteins [38,39]. Though LcrV is displayed on the surface of the bacterium and translocated via the T3SS, the antigen has also been reported to be shed into growth media *in vitro* [40]. A study conducted using a murine model of infection indicated that LcrV is detectable in serum and bronchoalveolar lavage fluid (BALF) in mice displaying symptoms of bubonic and pneumonic plague [41]. Since LcrV is essential for pathogenicity and appears to be shed during infection, it may serve as an important alternative biomarker for the diagnosis of plague [42–44].

While *Y. pestis* remains susceptible to many antibiotics, a growing number of resistant strains have been reported; and the ease of transferring resistance via plasmids is well established [45–47]. Furthermore, there is no FDA-approved vaccine for plague. A short incubation period, high mortality rates, and potential for mass infection through aerosolization warrant the development of novel countermeasures for the plague. In this study, prototype immunoassays were developed for the detection of LcrV and F1 for potential diagnosis of plague infections. Hybridoma cell lines producing mAbs against LcrV and F1 antigens were produced.

The resulting mAbs were evaluated for binding kinetics and used to develop sensitive immunoassay prototypes. Many mAb pair combinations were evaluated to develop LFIs and ELISAs for the detection of LcrV and F1. Surrogate clinical samples were used to determine the analytical sensitivity or LOD for the LFI prototypes. Pathogenic near neighbors and other Tier 1 bacterial Select Agents were used to begin to evaluate specificity of the LFI. The overall goal is for these prototypes to eventually be validated in a variety of sample matrices collected from plague patients followed by FDA approval.

Methods

Ethics statement

The use of Normal Human Serum has been reviewed by the Institutional Review Board at the University of Nevada, Reno (OHRP #IRB00000215). Normal Human Serum acquired from a commercial source has been classified as exempt human subject research (exemption 4) as i) no specimens will be collected specifically for this study and ii) there are no subject identifiers. As a consequence, the use of clinical samples in this project does not meet the criteria of human subject research as per 45 CFR 46 of the HHS regulations.

The use of laboratory animals in this study was approved by the University of Nevada, Reno Institutional Animal Care and Use Committee (protocol number 00024). All work with animals at the University of Nevada, Reno was performed in conjunction with the Office of Lab Animal Medicine, which adheres to the National Institutes of Health Office of Laboratory Animal Welfare (OLAW) policies and laws (assurance number A3500-01).

Monoclonal antibody (mAb) production

Animals were used in this study to produce reagents (mAbs) for the development of immunoassay assays. All animal work and husbandry were in the animal facility at the University of Nevada, Reno. Twenty female CD1 mice, 6–8 weeks old (Charles River Laboratories, Inc.), were immunized with either recombinant F1/LcrV fusion protein (F1-V), LcrV, or F1 (Biodefense and Emerging Infections Research Resources Repository [BEI Resources], Manassas, VA). Subcutaneous injections of recombinant F1-V, LcrV, or F1 in emulsions of Titermax Gold Liquid Adjuvant (TiterMax, Norcross GA) were performed with subsequent boosts at weeks 4 and 8. Immunizations of recombinant F1 were also performed using Freund's complete adjuvant (MilliporeSigma, Billerica, MA) via intraperitoneal injection with subsequent boosts using Freund's incomplete adjuvant (MilliporeSigma) at weeks 4, 8 and 12. The number of animals was selected to account for variability in the immune response, human error, and for any unforeseeable causes (i.e. death of animal). Sera samples were collected via submandibular or retro-orbital survival bleeds and titers were screened by indirect ELISA. A final boost of recombinant protein without adjuvant was administered intravenously three days prior to splenectomy. Euthanasia was performed by CO₂ asphyxiation and final bleeds were performed via cardiac sticks. Splenocytes from all mice were harvested and hybridoma cell lines were produced by standard technique using the P3X63Ag8.653 fusion partner [48]. Splenocytes from mice with the highest titers against the target antigen, as assessed by indirect ELISA, were prioritized to produce hybridoma cell lines. Remaining splenocytes were frozen down and stored in liquid nitrogen. Hybridoma cell lines were isolated through cloning by limiting dilutions. Cells were grown *in vitro* using Dulbecco's Modified Eagle's Medium (DMEM) containing fetal bovine serum (FBS) and conditioned media. Supernatant was collected and purified by protein A affinity chromatography yielding >10 mg/L purified mAbs.

Indirect ELISA

Microtiter plates (96-wells) were coated with recombinant protein (LcrV or F1) in phosphate buffered saline (PBS) overnight at room temperature. Plates were washed with PBS containing 0.05% Tween-20 (PBS-T) then blocked for 90 minutes at 37°C with PBS-T containing 5% non-fat milk (blocking buffer). Primary antibodies (mouse sera or purified mAbs) were diluted in blocking buffer and serial two-fold dilutions were performed across plates. Primary antibodies were incubated for 90 minutes at room temperature. Plates were washed with blocking buffer then incubated with horseradish peroxidase (HRP) labeled goat anti-mouse IgG antibody (Southern Biotech, Birmingham, AL) for 60 minutes at room temperature. Isolated mAbs were also analyzed using IgG subclass specific (IgG3, IgG1, IgG2a, IgG2b) goat anti-mouse secondary antibodies (Southern Biotech) for further characterization. Plates were washed with PBS-T and incubated with tetramethylbenzidine (TMB) substrate (Kirkegaard & Perry Laboratories, Inc., Gaithersburg, MD) for 30 minutes at room temperature. An equal volume of 1 M phosphoric acid (H₃PO₄) was used to stop the reaction, and colorimetric data was read at an optical density of 450 nm (OD₄₅₀).

Bacterial lysate preparation

At biosafety level 2 (BSL2), a glycerol stock of *Y. pestis* Harbin-35 (BEI Resources) was streaked onto a brain-heart infusion (BHI) agar plate and incubated at 28°C for 48 hours. An individual colony was picked, inoculated into tryptic soy broth (TSB), and grown overnight at 37°C shaking in 5% CO₂. Larger cultures were inoculated from the starter culture and grown for 48 hours at 37°C shaking in 5% CO₂. Bacterial cells were pelleted by centrifugation and resuspended in PBS. Cells were heat-inactivated at 80°C for 2 hours. Bacterial supernatant was 0.2 µm filtered. Bacterial cell lysate and supernatant were backplated onto BHI agar and incubated at 37°C for at least 72 hours to ensure no viable cells were present.

Additionally, bacterial lysates for *Y. pestis* KIM D19, *Y. pestis* A12 Derivative 6, *Y. pseudotuberculosis* IP2666, *Y. enterocolitica* WA, *Francisella tularensis* B38, *F. tularensis* LVS, *Bacillus anthracis* Ames-35, *Burkholderia pseudomallei* K96243, *B. pseudomallei* 1026B, and *B. pseudomallei* Bp82 were prepared as per instructed (BEI Resources). Bacterial lysates were heat inactivated and separated by cells and supernatant. *B. pseudomallei* strains K96243 and 1026B were propagated at biosafety level 3 (BSL3) and confirmed nonviable before removal to (BSL2) by a validated protocol. *Y. pestis* KIM D19, *Y. pestis* A12 Derivative 6, *Y. pseudotuberculosis* IP2666, *Y. enterocolitica* WA, *F. tularensis* B38, *F. tularensis* LVS, *B. anthracis* Ames-35, and *B. pseudomallei* Bp82 lysates were propagated at BSL2 as per protocol above. Inactivated bacterial cells were resuspended in PBS to an optimal density at 600 nm (OD₆₀₀) of 0.5.

Recombinant LcrV and F1 cloning and expression

Genes encoding LcrV and F1 were cloned into *Escherichia coli*, expressed and purified. The F1 encoding gene (*caf1*) and *lcrV* were amplified by polymerase chain reaction (PCR) from the *Y. pestis* Harbin-35 lysate, using primers shown in S1 Table. The *caf1* gene was void of the first 63 base pairs which encodes for a cleaved signal peptide [49]. Each gene was cloned into the pQE-30 Xa Vector (Qiagen, Hilden, Germany) by Gibson Assembly (New England Biolabs (NEB), Ipswich, MA). Plasmids were sequence verified and transformed into *E. coli* M15 for protein expression. *E. coli* containing expression plasmids were grown at 37°C to an optimal density at OD₆₀₀ of 0.6 before inducing protein expression by the addition of isopropyl β-D-1-thiogalactopyranoside (IPTG) at an end concentration of 1mM. Induced cultures were grown at 37°C for 12–16 hours. Bacterial cell pellets were collected by centrifugation then lysed with

BugBuster 10X Protein Extraction Reagent (MilliporeSigma) and sonication. The soluble fraction for both were purified using Protino Ni-TED resin (Macherey-Nagel, Duren, Germany).

Western blot

A standard Western blot procedure was performed using semidry blotting. 6x reducing or non-reducing Laemmli loading buffer was added to bacterial lysate. The reduced sample was then boiled for 10 minutes to denature the proteins. Samples were separated on a 10% sodium dodecyl sulfate (SDS) gel, and proteins were transferred to a nitrocellulose membrane (Bio-Rad Laboratories, Hercules, CA). HRP-labeled LcrV mAbs were used to probe the membrane directly. Unlabeled F1 mAbs were used to probe the membrane, followed by an HRP-labeled goat anti-mouse Ig for detection. Signal was developed using SuperSignal™ West Femto Maximum Sensitivity Substrate (ThermoFisher Scientific, Grand Island, NY) and imaged using a ChemiDoc XRS imaging system (Bio-Rad Laboratories).

LFI

LFIs were initially constructed using Fusion-5 matrix membrane (GE Healthcare, Piscataway, NJ), FF120HP nitrocellulose membrane (GE Healthcare) and C083 cellulose fiber sample pad strips (Millipore Sigma). FF120HP membranes were striped with unlabeled antibodies using the BioDot XYZ platform (BioDot, Irvine, CA). Purified *Y. pestis* mAbs were striped at 1 mg/mL and served as the test line. Unlabeled goat anti-mouse Ig (Southern Biotech) were striped serving as the control line. All mAbs were conjugated to 40 nm colloidal gold particles (DCN Diagnostics, Carlsbad, CA), blocked with bovine serum albumin and concentrated to an optical density of 10 at 540 nm. Stability of the mAb conjugates were tested by stability in high salt conditions. Colloidal gold conjugated mAbs were spotted roughly 8mm from the top of the Fusion-5 matrix membrane prior to running the assay and served as the detection antibody. Initial screening was done using all possible mAb pairs for LcrV and F1. A single concentration of recombinant protein (100 ng/mL) was used to evaluate mAb pairing. Samples of 40 μ L were loaded onto the sample pad then placed in a well containing 150 μ L of chase buffer only. Each prototype was run in parallel with chase buffer only, as a negative control. Test line intensity was read promptly after 20 minutes using the ESE Lateral Flow Reader (Qiagen). Top performing pairs were then down selected using a concentration of 1 ng/mL of recombinant protein.

Top LFI prototypes were optimized for testing using human sera. Recombinant protein (LcrV or F1) was spiked into six lots of pooled normal human sera ([NHS], Bioreclamation IVT, Westbury NY & Innovative Research, Novi MI) and evaluated for signal intensity and non-specific background signal. LFI components optimized include conjugate release pads, nitrocellulose membranes, wicking pads, chase buffers, striping concentrations, gold conjugate diluents and sample pre-treatment steps (S2 Table). The final prototypes were constructed using UniSart CN140 nitrocellulose membrane (Sartorius, Germany), CFSP203000 absorbent pad, and conjugate pad grade 8951 (Ahlstrom, Finland). F127 and 10G surfactants were added to the gold diluent for the LcrV and F1 prototypes respectively to help with the release of the conjugate from the conjugate pad. Mouse IgG was added to the human serum samples as a pretreatment step to prevent human anti-mouse antibody (HAMA) interference [50].

Antigen-capture ELISA

The top eight performing mAbs ranked by LFI testing were screened to develop antigen-capture ELISAs. Microtiter plates were coated overnight with 1 μ g/mL capture mAb. After blocking, recombinant protein (F1 or LcrV) was diluted into blocking buffer and serial two-fold

dilutions were performed across plates. Detection antibody at 0.1 µg/mL was incubated for 60 minutes at room temperature. HRP labeling of mAbs was performed using EZ-Link Plus Activated Peroxidase (ThermoFisher Scientific). Plates were washed with PBS-T and incubated with TMB substrate for 30 minutes at room temperature. An equal volume of 1M H₃PO₄ was used to stop the reaction, and colorimetric data was read at OD₄₅₀.

Checkerboard ELISAs were performed using the top two mAb pairs to optimize concentrations of capture and detection mAbs. Optimization was performed using two-fold serial dilutions of either the capture or detection mAbs in independent experiments. The capture mAbs was first optimized by using concentrations ranging from 0.078–10 µg/mL with 1 µg/mL detection mAb. Capture mAb concentrations were chosen based on signal intensity and minimal background. The selected capture mAb concentrations were used to optimize the detection mAbs from a range of 0.0078–1 µg/mL. The optimized ELISA conditions were selected based on the lowest LOD defined as the concentration at two-fold background signal. The top two mAb pairs for each antigen were evaluated to determine the theoretical ELISA limit of detection defined as two-fold background signal.

Surface plasmon resonance (SPR)

SPR experiments were conducted on the Biacore X100 instrument using the His Capture format (GE Healthcare). A CM5 chip surface was prepared using the His Capture Kit as per manufacturer's recommendation. For each cycle, his-tagged recombinant protein (LcrV or F1) diluted into HBS-EP+ buffer (GE Healthcare) was immobilized onto the anti-His capture surface. LcrV was immobilized at a concentration of 5 µg/mL and F1 was immobilized at a concentration of 1 µg/mL. Antigen capture was performed at 5 µL/second for 60 seconds followed by 120 second stabilization. These conditions were established for optimal kinetic analyses of each mAb. Full kinetic analyses were performed by injecting each purified mAb for 7 cycles at a concentrations range of 0.5–50 µg/mL over the LcrV or F1 surface for 120 seconds followed by a dissociation period of 240 seconds at 30 µL/second. The anti-His capture surface was regenerated between each cycle using 10 mM glycine pH 1.5 (GE Healthcare) for 30 seconds at 10 µL/second. Binding kinetics and affinity were evaluated using a bivalent model on the Biacore X100 Evaluation Software (GE Healthcare).

Results

Hybridoma production and mAb reactivity

In order to develop antigen-capture immunoassays for the detection of LcrV and F1, a large panel of mAbs were isolated and evaluated to determine the optimal conditions for assay performance. Titermax Gold or Freund's adjuvants were combined with antigens and used for immunization [51,52]. Twenty-two hybridoma cell lines that produce mAbs against *Y. pestis* LcrV or F1 were isolated (Table 1). MAb reactivity was confirmed by indirect ELISA to recombinant F1 or LcrV proteins. Additional mAbs were isolated from mice immunized with the F1-V fusion protein; however, these mAbs were only reactive to the F1-V fusion protein and not reactive to the individual proteins. Subclass specific secondary antibodies were used to characterize each mAb subclass, and all antibodies were determined to be members of the IgG1, IgG2b, or IgG2a subclass (Table 1). These antibody subclasses are preferred over the IgG3 subclass in the development of antigen-capture immunoassays as the IgG3 subclass can self-associate resulting in increased background signal and potential false positive reactions [53].

Western blot analysis probing *Y. pestis* Harbin-35 lysate determined mAb reactivity against the two *Y. pestis* proteins. High density bands were detected at the expected molecular weight

Table 1. Monoclonal antibody (mAb) library against *Y. pestis* LcrV and F1 antigens.

Antigen	mAb	Immunization	Subclass	
LcrV	2B2	F1-V	IgG2a	
	4E8	LcrV	IgG2a	
	5D3	LcrV	IgG1	
	6E5	LcrV	IgG1	
	6F10	LcrV	IgG1	
	8F3	LcrV	IgG1	
	8F7	LcrV	IgG2a	
	8F10	LcrV	IgG1	
	F1	3A2	F1-V	IgG2a
		3F2	F1	IgG1
4E5		F1	IgG2a	
4F12		F1	IgG1	
5E10		F1	IgG2a	
9B7		F1	IgG1	
10D9		F1	IgG1	
10E3		F1	IgG1	
11B8		F1	IgG2a	
11C7		F1	IgG1	
12B6		F1	IgG2a	
12E10		F1	IgG2a	
12F5		F1	IgG2b	
15C4		F1	IgG2a	

<https://doi.org/10.1371/journal.pntd.0010287.t001>

of roughly 40 kDa indicating reactivity with monomeric LcrV protein (Fig 1A) [54]. Reactivity is observed at higher molecular weights, indicating that both monomeric and multimeric forms are produced in bacterial culture [54]. MAbs 4E8 and 5D3 had limited reactivity to the non-reduced protein as well as the multimeric forms suggesting reactivity to linear epitopes that are more available in reducing conditions (Fig 1B). MAbs isolated against F1 showed differing levels of reactivity to the monomeric F1 antigen in the reduced Western blot (Fig 2A). The non-reduced Western blot analysis showed reactivity of the F1 mAbs against the assembled F1 capsule which resulted in an expected laddering pattern (Fig 2B) [55]. Reducing conditions disrupt disulfide bonds as heat disrupts other protein-protein interactions; therefore these conditions disassemble the F1 capsule's native polymeric structure. MAb 3A2 was isolated from a mouse immunized with the F1-V fusion protein and showed preferential reactivity to the monomeric structure and had low reactivity to the assembled capsule. Inversely, mAbs 9B7 and 12F5 showed limited reactivity to the reduced bacterial lysate and were more reactive against higher molecular weight F1 multimers present in the non-reduced lysate (Fig 2B). Reactivity of mAbs 9B7 and 12F5 may suggest binding only occurs to a specific epitope formed in the F1 capsule between at least three or more subunits (>46.5 kDa).

Binding affinity and kinetics by surface plasmon resonance (SPR)

Characterization of the mAbs in each library included analysis of binding kinetics by SPR. Experiments were performed in triplicate and evaluated using a bivalent binding model. The association rate (k_a), dissociation rate (k_d), and equilibrium dissociation constant (K_D ; $K_D = k_d/k_a$) are reported in Table 2. LcrV mAbs displayed a narrow range of equilibrium dissociation constants (0.3–4.5 nM). F1 mAbs had a larger range of 0.002–250 nM. Interestingly,

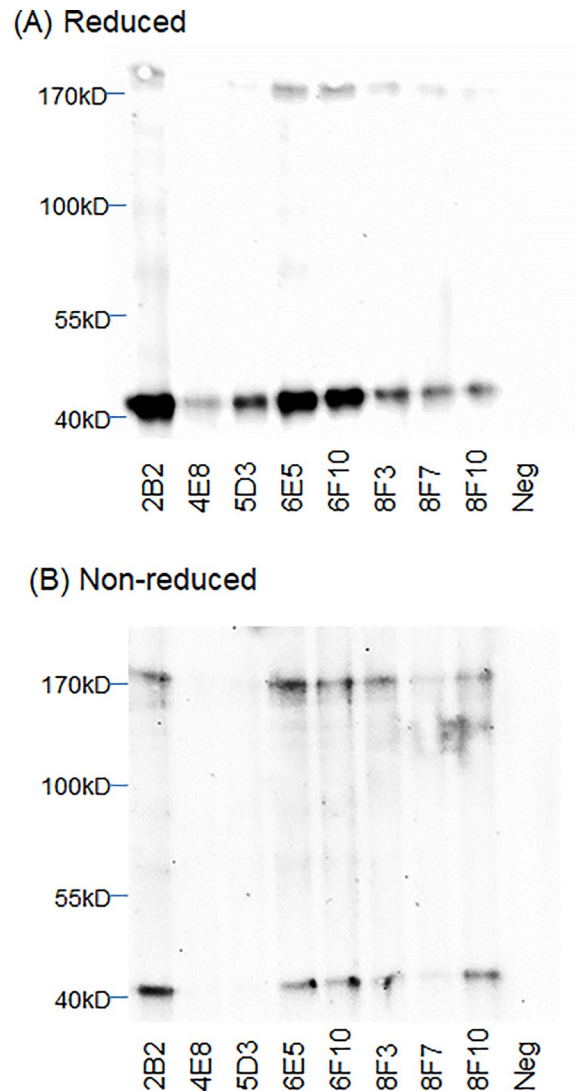


Fig 1. Western blot analysis of anti-LcrV monoclonal antibodies (mAbs) against *Yersinia pestis* Harbin-35 lysate. Horseradish peroxidase (HRP) conjugated LcrV mAbs (1 $\mu\text{g}/\text{mL}$) were used to probe (A) reduced and (B) non-reduced *Y. pestis* Harbin-35 bacterial lysate (1.5×10^6 cells/lane) by direct Western blot.

<https://doi.org/10.1371/journal.pntd.0010287.g001>

mAbs 2B2 and 3A2 were isolated from mice immunized with the F1-V fusion protein. 2B2 displayed a high affinity to recombinant LcrV ($K_D = 2.6$ nM); however, 3A2 displayed the poorest affinity to recombinant F1 ($K_D = 250$ nM).

LFI development and optimization

The library of mAbs were evaluated as capture and detection components for the development of LFI prototypes. MAb pairs were quantitatively ranked based on the signal intensity at the test line when analyzing a sample containing 100 ng/mL of recombinant protein (LcrV or F1) spiked into chase buffer minus nonspecific signal when chase buffer alone was analyzed (S3 and S4 Tables). Though LFIs are generally evaluated by visual detection, the use of Qiagen ESE Lateral Flow Reader provided a standardized measure to minimize human variability and

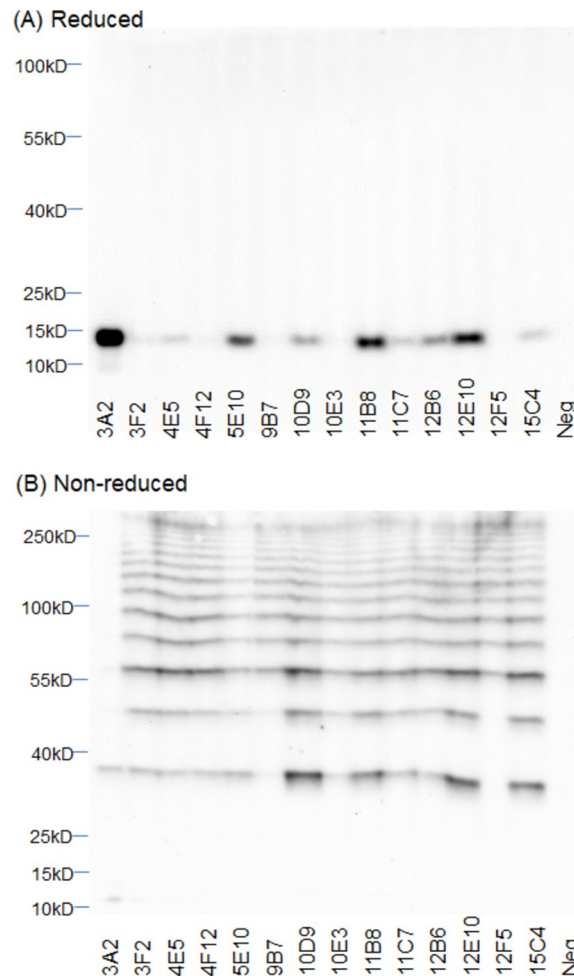


Fig 2. Western blot analysis of anti-F1 monoclonal antibodies (mAbs) against *Yersinia pestis* Harbin-35 lysate. Anti-F1 mAbs (1 $\mu\text{g}/\text{mL}$) were used to probe (A) reduced and (B) non-reduced *Y. pestis* Harbin-35 bacterial lysate (1.5×10^6 cells/lane) by indirect Western blot. HRP-conjugated goat anti-mouse Ig was used for detection of F1 mAb binding.

<https://doi.org/10.1371/journal.pntd.0010287.g002>

error. Visual LOD is estimated to have an intensity between 15–30 $\text{mm}^* \text{mV}$ among various LFIs developed in our laboratory. The mAb pairs were then down selected for detection of 1 ng/mL recombinant protein (Table 3). The top four performing pairs (capture/detection) were evaluated for detection of LcrV in bacterial lysate (S1 Fig). MAb pair 8F10/2B2 was highly reactive to bacterial lysate. This pair, however, consistently had nonspecific reactivity with control, prompting the evaluation of the next top performing pair (8F10/6F10). Further optimization is warranted to minimize nonspecific reactivity as these results together suggest 8F10/2B2 is more analytically sensitive when detecting native protein despite 8F10/6F10 having similar results with recombinant protein (Table 3). The top pair for F1 detection was 11C7/3F2 when evaluated with 1 ng/mL recombinant F1 protein (Table 3). S5 Table shows additional F1 LFI prototypes that displayed reactivity in chase buffer alone.

Testing complex matrices such as human sera often lead to assay signal loss and nonspecific binding described as matrix effects [56]. To account for interference of the matrix on downstream applications, the top LFI prototypes were further optimized for assaying human serum. The LOD was defined as the minimum concentration of recombinant protein at which a

Table 2. Affinity and kinetics analysis of *Y. pestis* mAbs by surface plasmon resonance.

Antigen	mAb	$k_a \times 10^3 (M^{-1}s^{-1})$	$k_d \times 10^{-3} (s^{-1})$	$K_D (nM)$
LcrV	2B2	52	0.14	2.6
	4E8	210	0.78	3.7
	5D3	65	0.22	3.4
	6E5	120	0.54	4.5
	6F10	140	0.58	4.1
	8F3	93	0.17	1.9
	8F7	100	0.18	1.8
	8F10	250	0.074	0.3
F1	3A2	5.6	1.4	250
	3F2	65	0.48	7.4
	4E5	250	0.39	1.6
	4F12	91	1.8	19
	5E10	230	0.12	0.5
	9B7	42	0.45	11
	10D9	36	0.048	1.3
	10E3	100	0.054	0.5
	11B8	170	0.17	1.0
	11C7	180	0.91	5.2
	12B6	110	0.00026	0.002
	12E10	83	0.23	2.8
	12F5	170	13	79
	15C4	210	0.13	0.6

<https://doi.org/10.1371/journal.pntd.0010287.t002>

positive signal is observed in spiked pools of normal human sera (NHS). In this study, a positive signal was defined as an intensity reading greater than 20 mm*mV using the Qiagen ESE Lateral Flow Reader. Due to sample variability, difference in assay performance was observed between each lot of pooled human serum. Six different pools of NHS were used to optimize each LFI prototype for nonspecific background signal. Then the pools were spiked with recombinant protein and used to determine the LOD of the LFI prototypes to account for possible matrix effects on signal intensity. The LOD of the 8F10/6F10 LFI was estimated to be 2 ng/mL when recombinant LcrV was spiked into NHS (Lot NHS207) (Fig 3A). The LOD of the 11C7/3F2 LFI was estimated to be 1 ng/mL when recombinant F1 was spiked into NHS (lot NHS207) (Fig 3B). Despite high analytical sensitivity to each antigen, differences of assay signal were

Table 3. Assay sensitivity of the top 4 mAb pairs (LcrV or F1) by lateral flow immunoassay.

Antigen	Capture mAb	Detection mAb	OD (mm*mV) 1 ng/mL antigen	OD (mm*mV) Chase Buffer only
LcrV	8F10	6F10	56	0
	8F10	2B2	53	0
	8F10	6E5	51	0
	8F7	6F10	26	0
F1	11C7	3F2	115	0
	11C7	15C4	93	0
	4E5	3F2	89	0
	10D9	3F2	57	0

<https://doi.org/10.1371/journal.pntd.0010287.t003>

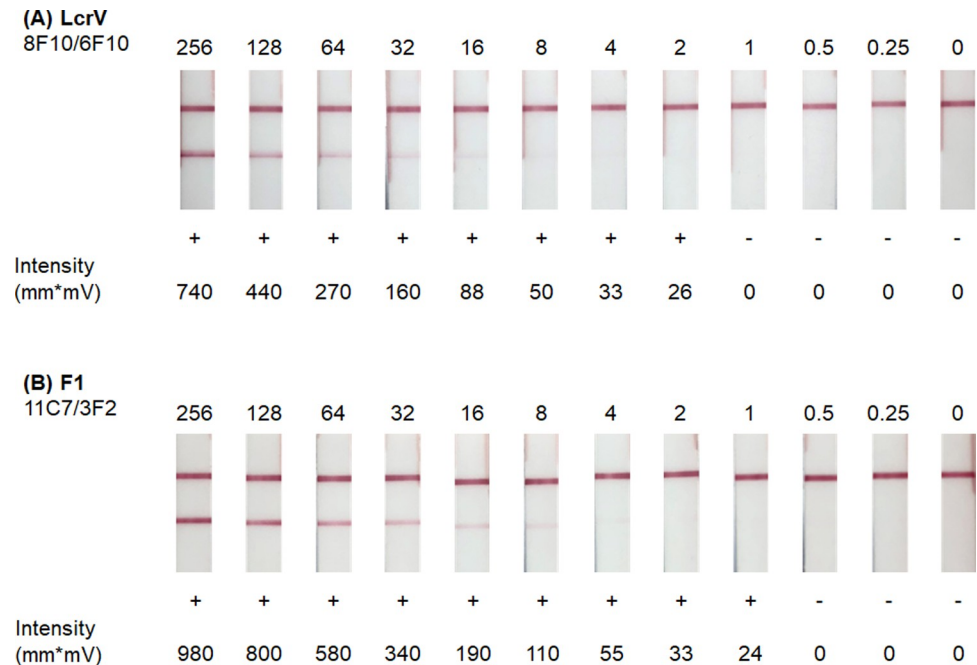


Fig 3. Sensitivity of *Y. pestis* lateral flow immunoassays (LFI) using recombinant LcrV and F1. LFI prototypes were tested with recombinant (A) LcrV and (B) F1 serial diluted into pooled normal human serum ranging from 0.25 to 256 ng/mL. Assay signal was evaluated and quantitated by optical density using a Qiagen ESE reader. Intensity ≥ 20 mm*mV scores as positive.

<https://doi.org/10.1371/journal.pntd.0010287.g003>

observed between the six pools of NHS (S2 and S3 Figs). The aggregate LOD was determined as the lowest concentration which consistently resulted in positive LFIs among the pools of NHS. The LcrV and F1 prototypes produced LODs of roughly 1 ng/mL. Detection of both antigens in pooled NHS #28614 appeared slightly reduced (S2 Fig) and illustrates the variation in signal intensity that can occur when testing within different lots of pooled human serum.

Generation of a multiplexed LcrV/F1 assay

To detect potentially all pathogenic isolates of *Y. pestis*, a multiplexed LFI was developed. The prototype was constructed with two test lines, one specific for LcrV (8F10/6F10) and one for F1 (11C7/3F2). Initial specificity testing of the dual LFI prototype was performed using bacterial lysates from Select Agent exempt strains of *Y. pestis*, clinically relevant near neighbors, and other Tier 1 bacterial Select Agents (Fig 4). Cell lysates were adjusted to an OD₆₀₀ of 0.5. *Y. pestis* Harbin-35 and KIM19 strains were positive for LcrV and F1. *Y. pestis* A12 Derivative 6, an LcrV⁻ strain, was positive only for F1. *Y. pseudotuberculosis* IP2666 lysate was positive for LcrV, but *Y. enterocolitica* was negative for LcrV. High levels of homology attribute to some degree of mAb cross-reactivity to LcrV of near neighbors [42,57]. Additionally, all other Tier 1 bacterial Select Agents were negative for both LcrV and F1.

Antigen-capture ELISA development and optimization

The top eight mAbs ranked by LFI were used to develop a quantitative antigen-capture ELISAs for the detection of *Y. pestis* antigens. ELISA mAb pairs were initially evaluated using 1 μ g/mL capture mAb and 0.1 μ g/mL detection mAb. To compare the performance of each mAb pair, antigen concentrations at five-fold background signal were determined from a linear

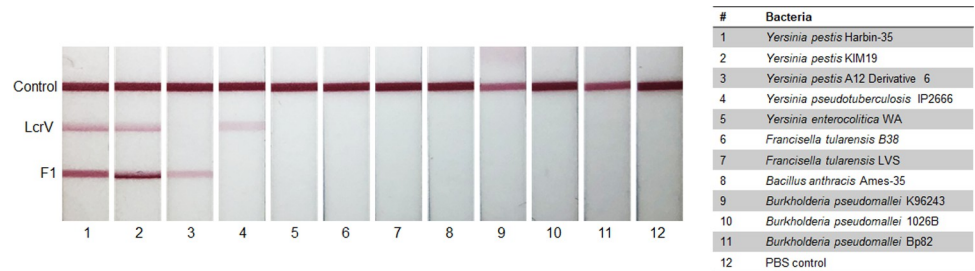


Fig 4. Specificity testing of dual *Yersinia pestis* lateral flow immunoassay (LFI) against clinically relevant bacterial panel. The dual LFI prototype containing test lines specific for LcrV (8F10/6F10) and F1 (11C7/3F2) was tested against a panel of bacterial lysates. Bacterial lysate (50 μ L at OD₆₀₀ = 0.5) was applied onto the conjugate pad and chased with buffer. LFIs were imaged after 20 minutes.

<https://doi.org/10.1371/journal.pntd.0010287.g004>

regression plot generated from a two-fold serial dilution of each antigen (S4 Fig). This value (five-fold background) was selected to account for possible background signal caused by the mAb pairing. The top two performing mAb pairs for each antigen were optimized for capture and detection conditions by checkerboard ELISAs (Table 4). The theoretical ELISA LODs (defined as two-fold background signal) for each assay were determined using recombinant protein spiked into buffer and reported in Table 4 and S5 Fig. LcrV was detected at 74 pg/mL by 6E5/8F10 and F1 was detected at 61 pg/mL by 11B8/11C7.

Discussion

The quick progression of plague infections warrants the need for sensitive, specific, and rapid diagnostic tools. Though most infections lead to bubonic plague, the more severe forms of the infection present with nonspecific clinical symptoms that can be challenging to distinguish from many other diseases. Commercially available LFIs have been developed for the detection of the F1 antigen and is used for patient screening, however no product is currently FDA approved to diagnose plague [18,20]. F1 encapsulates the bacteria and is shed; however, F1⁻ isolates have been identified and are fully virulent making the biomarker inadequate for diagnosing all plague infections [25,33]. To combat the potential of widespread infections, an RDT capable of detecting all pathogenic strains of *Y. pestis* is imperative. Through the isolation of a library of mAbs reactive to F1, as well as LcrV, we have developed assays for the detection of various pathogenic *Yersinia* species which may prove to be useful on multiple fronts.

The success of *Y. pestis* as a pathogen may be attributed to its genetic diversity. Widespread pandemics have been traced to three global biovars of *Y. pestis* (*antiqua*, *medievalis*, and *orientalis*). The *lcrV* gene is conserved among the biovars virulent in humans [54]. Polymorphisms in *lcrV* have been observed in the biovar *microtus* [58]. Some polymorphisms occur in critical

Table 4. Limit of detection of enzyme-linked immunosorbent assays using recombinant LcrV and F1 antigens in buffer.

Antigen	Capture mAb	[Capture mAb] (μ g/mL)	Detection mAb	[Detection mAb] (μ g/mL)	LOD* (pg/mL)
LcrV	6E5	2.5	8F10	0.13	74 \pm 7.9
	6F10	2.5	8F10	0.063	75 \pm 4.0
F1	10D9	2.5	11C7	0.13	100 \pm 41
	11B8	1.3	11C7	0.13	61 \pm 2.0

*LOD defined as the concentration at two-fold background signal

<https://doi.org/10.1371/journal.pntd.0010287.t004>

regions impacting LcrV to form multimers, suggesting the attenuation of certain biovars in humans [54]. In addition to polymorphisms in *lcrV*, various isoforms of the F1 antigen exist due to point mutations [59,60]. The NT1 isoform (Ala⁴⁸ Phe¹¹⁷) is most common and is expressed by the three global strains responsible for human infections [59]. Moreover, the adaptive immune response elicited by the NT1 isoform are cross-reactive to the NT2 (Ser⁴⁸ Phe¹¹⁷) and NT3 (Ala⁴⁸ Val¹¹⁷) isoforms suggesting these amino acid substitutions may not affect the binding of the described mAbs [61]. *Y. pestis* Harbin-35 and KIM D19 strains are included within biovar *medievalis* and maintain the three plasmids associated with virulence (pCD1, pPCP1, pMT1), but are attenuated due to the deletion of the *pgm* locus, which encodes a segment of the chromosome that includes a pathogenicity island [62]. The *pgm* locus encodes for various iron-regulated proteins necessary for bubonic and pneumonic plague infections [63]. Unlike most laboratory strains, Harbin-35 and KIM D19 maintain the pCD1 plasmid and LcrV expression. The A12 D6 strain is included within the biovar *orientalis* and is lacking the entire pCD1 plasmid. mAbs isolated in this study show reactivity to *Y. pestis* Harbin-35, KIM D19, and A12 D6 proteins which suggest mAb binding may be against all human pathogenic strains of *Y. pestis* (Figs 1–2 & 4). Further characterization of the mAb panel should be performed to confirm reactivity among all pathogenic *Y. pestis* strains.

Binding kinetics derived from SPR demonstrate that most of the mAbs produced in this study possess high affinity to their targets (Table 3). In general, higher affinity mAbs are preferred in immunoassays to achieve optimal analytical sensitivity which should result in improved clinical sensitivity; however, the mAb pairs which performed well in LFI and ELISA formats did not necessarily have the highest affinity or superior kinetics. Initial screening of LcrV mAbs by ELISA indicated that the pairing of high affinity mAbs 8F7 and 8F10 resulted in LODs 10 to 20-fold less sensitive than 8F10 and either 6E5 or 6F10, mAbs with lower degrees of affinity (Table 2; S4 Fig). Likewise, the mAbs used in the optimized F1 ELISAs (10D9, 11B8, and 11C7) were ranked among the middle for binding affinity (K_D). Additionally, mAb 12B6 had binding affinity over 2 logs greater ($K_D = 0.002$ nM) than the other mAbs in the panel but did not perform well in the antigen-capture format. Overall, the mAbs used to develop the sandwich assays all displayed dissociation constants less than 10 nM. These results exemplify that in addition to having high affinity, mAbs used in antigen-capture immunoassays require pairing synergy.

Interestingly, the top performing mAb pairs in the LFI format were not the same as the ELISA. Evaluation of LFI and ELISA mAb pairs for Ebola glycoprotein and *F. tularensis* in our laboratory have also shown differences between the two formats [64,65]. Though both LFIs and ELISAs are antigen-capture immunoassays, there are notable differences in the assay formats. ELISAs reach binding equilibrium with long incubation periods, minimize nonspecific binding with several wash steps, and are more sensitive due to enzymatic signal amplification. However, the ELISA format is less accessible in low-technology settings such as in the field or in developing countries due to laboratory equipment requirements and storage of temperature-sensitive reagents. In contrast, LFIs utilize capillary flow to apply reagents systematically without intermediate washing steps, are self-contained within a single dipstick, and produce results in less than 20 minutes by the colorimetric sensing of gold-nanoparticle aggregates, optimal for visual detection by the human eye.

The RDT immunoassay prototypes developed in this study had analytical sensitivities within appropriate levels for assaying serum. Levels of F1 in patient serum can range from 4–50,000 ng/mL [66]. Concentrations of soluble LcrV in human samples have yet to be determined, but a mouse model of infection indicates serum concentrations of LcrV are between 6–26.5 ng/mL 48 hours post-inhalational exposure [41]. To determine the diagnostic potential of LcrV and F1, further studies will need to be conducted within the 48 hours of exposure as

this window is crucial for administering treatment for patient survival. The ELISAs developed in this study would be useful in quantifying LcrV and F1 in plague patient samples to further validate each diagnostic target. Additionally, the ELISA format may also be important in outbreak settings to allow for high throughput screening of patient samples. Furthermore, the top mAb pair for detecting LcrV by LFI was evaluated in a vertical flow immunoassay (VFI) format. The mini VFI prototype can detect as low as 25 pg/mL LcrV [67].

Y. pestis can invade the bloodstream and be detected within days of exposure, making blood a common test matrix among the three forms of plague. The LFI prototypes were optimized for serum as it is similar to whole blood and can cause matrix effects, or interference by components present in the clinical sample at the test line. Matrix effects were evident in testing both the LcrV and F1 LFIs as pools of normal human serum resulted in varying signal intensity. The LOD results for both the LcrV and F1 prototypes roughly 1 ng/mL. Additionally, the optimized LFI prototypes were able to analyze up to 50 μ L of neat human sera with a minimal degree of pre-treatment. The tested assay protocol includes a sample preparation step in which mouse IgG was added to prevent HAMA interference. However, mouse IgG could be integrated into the sample pad prior to finalization of the LFI along with separation pads to allow for whole blood testing. Furthermore, the LFI prototypes described should be evaluated using other clinical matrices such as sputum or pus as these may be more clinically relevant for pneumonic and bubonic infections, respectively.

Plague remains a modern threat to public health, and LFIs are ideal tools for detecting and limiting the spread of infections. In addition to the risk of naturally occurring plague, *Y. pestis* has been used as a biological weapon. The use of *Y. pestis* in medieval siege warfare has been well documented, and in modern times, plague-infected fleas were disbursed by the Japanese army in China during World War II [68]. Several countries, including the United States of America and the former Soviet Union, have investigated the utility of *Y. pestis* as a bioweapon [9]. Further investigation of *Y. pestis* as a biological weapon is no longer permitted under a treaty signed at the Biological Weapons Convention in 1972. Nonetheless, continued development of countermeasures against *Y. pestis* are warranted in defense of nefarious actions. Of concern is the intentional release of an F1⁻ strain as a bioterrorism tactic, as the F1 antigen is primarily regarded as a diagnostic and vaccine target [69–74]. The multiplexing of assays detecting LcrV and F1 increases the diagnostic ability of a *Y. pestis* RDT, as it may be capable of detecting all pathogenic *Y. pestis* strains including those found to be F1 deficient. The dual assay shows high specificity to *Y. pestis* without cross-reacting with other Tier 1 Select Agents with similar symptoms. It was anticipated that the LcrV/F1 prototype would be positive for LcrV *Y. pseudotuberculosis* as the homology is 97% compared to *Y. pestis* [75]. In cases where plague is suspected, a positive result for either F1 or LcrV should prompt immediate treatment [76]. More specificity testing needs to be performed using these prototypes with an increased panel of microbes known to present with similar symptoms. The prompt detection of all pathogenic *Y. pestis* is critical for minimizing casualties during naturally occurring outbreak or a potential bioterrorism act. Further evaluation on clinical samples collected from plague patients is needed to fully validate this multiplexed LFI.

While the immunoassay prototypes developed in this study were designed with patient samples in mind, a secondary use would be to evaluate animal populations and vectors for the presence of *Y. pestis*. As a zoonotic disease, plague surveillance requires the monitoring of natural animal reservoirs and associated vectors. Current methods of surveying wild populations include serological testing of sentinel animals, such as coyotes, which prey on smaller mammals [77]. Though coyotes do not present with symptoms, they do elicit an immune response to *Y. pestis* antigens [78]. The downside of serological surveillance is the persistence of antibodies long after exposure, meaning that a positive response may not be indicative of an active infection. Though expression of LcrV

and F1 are regulated by temperature, leaky expression of LcrV at 26°C has been observed [79]. This leaky expression should be evaluated as a mean to detect *Y. pestis* in vectors such as fleas. Screening of small mammals and vectors could be conducted using an LFI in the field to gain more data regarding the prevalence of *Y. pestis* in these reservoir populations.

In addition to use in a diagnostic assay, exogenous antibodies have shown to be effective in protecting from and treating plague infections when administered pre- and post-exposure. In a mouse model of pneumonic plague, F1 specific IgG mAbs were able to confer protection when administered prophylactically [80]. Additionally, three human mAbs (one against F1, two against LcrV) isolated by naïve human phage displayed Fab libraries demonstrate some protection for bubonic plague in mice [81]. LcrV and F1 mAb cocktails do have synergy when administered together [82]. LcrV subunits form pentamers at the tip of the T3SS at the cell surface [36,83]. LcrV in this pentameric structure is associated with immunosuppression properties and have shown to elicit a more protective response in vaccine studies [37,84]. Testing the therapeutic potential of this large panel of *Y. pestis* mAbs in an animal model of infection may result in the development of additional treatment options for plague patients.

Monoclonal antibodies, specific to LcrV and F1, were used to develop antigen-capture LFIs and ELISAs with high analytical sensitivity. The LFI prototypes resulted in LODs of roughly 1 ng/mL for both LcrV and F1 when assaying antigen spiked into normal serum. The ELISAs were able to achieve an analytical sensitivity in the range of 61–74 pg/mL, at this point testing was only preformed in assay buffer. The detection of the F1 antigen is widely used to diagnose plague infections, however mutant strains of *Y. pestis* lacking the F1 antigen have been identified. Initial inclusivity/exclusivity studies of the multiplexed LFI demonstrates that the inclusion of a second antigen, LcrV, should improve the performance of the RDT. The LcrV antigen is crucial for virulence and may be used as an alternative marker of plague. Further evaluation of LcrV is warranted and can be accomplished using the tools developed in this study. In addition, side-by-side analyses of the assays developed here with other plague assays is a logical next step in order to rank performance. Finally, the immunoassays developed hopefully will be diagnostically useful and there could be potential of the mAbs being further developed into therapeutics, thereby assisting in the control of future plague outbreaks.

Supporting information

S1 Fig. Top four LcrV LFI prototypes tested with (A) PBS or (B) *Y. pestis* Harbin-35 lysate for the detection of native antigen. Test lines were sprayed at 1 mg/mL and 5 uL of gold conjugated mAb ($OD_{540} = 10$) was applied.

(PDF)

S2 Fig. LFI prototypes (8F10-capture/6F10-detection) were tested with recombinant LcrV in six pools of normal human serum. Each panel represent a different lot of pool serum from (A-C) Bioreclamation IVT or (D-F) Innovative Resources. Lot numbers are provided for each panel. Assay signal was evaluated and quantitated by optical density using a Qiagen ESE reader. Intensity ≥ 20 mm*mV scores as positive.

(PDF)

S3 Fig. F1 prototypes (11C7-capture/3F2-detection) were tested with recombinant F1 in six pools of normal human serum. Each panel represent a different lot of pool serum from (A-C) Bioreclamation IVT or (D-F) Innovative Resources. Lot numbers are provided for each panel. Assay signal was evaluated and quantitated by optical density using a Qiagen ESE reader. Intensity ≥ 20 mm*mV scores as positive.

(PDF)

S4 Fig. Preliminary screen to identify top performing antigen-capture ELISA mAb pairs. Values shown are the concentrations of (A) recombinant LcrV and (B) recombinant F1 in ng/ml at five times background for each mAb pair. The values represent the mean of two independent ELISAs (each performed in biological triplicates).
(PDF)

S5 Fig. Antigen-capture ELISAs were performed to determine the limits of detection (LOD) for recombinant (A & B) LcrV and (C & D) F1. LODs were calculated using the linear regression of the optimized ELISA conditions to determine the concentration of recombinant protein in ng/ml at two-fold background. The values represent means of three independent ELISAs (each performed in biological triplicates).
(PDF)

S1 Table. Primers for cloning LcrV and F1 genes from *Y. pestis* Harbin-35 into the pQe-30 Xa vector.
(PDF)

S2 Table. Summary of lateral flow immunoassay components evaluated.
(PDF)

S3 Table. Preliminary assay sensitivities of top mAb pairs by LFI for LcrV at 100 ng/mL.
(PDF)

S4 Table. Preliminary assay sensitivities of top mAb pairs by LFI for F1 at 100 ng/mL.
(PDF)

S5 Table. Preliminary assay sensitivities of top mAb pairs by LFI for F1 at 1 ng/mL.
(PDF)

Acknowledgments

We would like to acknowledge the guidance provided through the DCN Dx Custom Lateral Flow training for suggestions for optimizing LFI's.

Author Contributions

Conceptualization: Derrick Hau, Brian Wade, Sujata G. Pandit, Marcellene A. Gates-Hollingsworth, Peter N. Thorkildson, Kathryn J. Pflughoeft, David P. AuCoin.

Data curation: Derrick Hau, Brian Wade, Chris Lovejoy, Sujata G. Pandit, Dana E. Reed, Haley L. DeMers, Heather R. Green, Emily E. Hannah, Megan E. McLarty, Cameron J. Creek, Chonnikarn Chokapirat, Jose Arias-Umana, Garrett F. Cecchini, Teerapat Nualnoi.

Formal analysis: Derrick Hau, Brian Wade, Chris Lovejoy, Dana E. Reed.

Funding acquisition: Marcellene A. Gates-Hollingsworth, David P. AuCoin.

Investigation: Derrick Hau, Sujata G. Pandit, David P. AuCoin.

Methodology: Derrick Hau, Brian Wade, Chris Lovejoy, Sujata G. Pandit, Dana E. Reed, Teerapat Nualnoi, Marcellene A. Gates-Hollingsworth, Peter N. Thorkildson, Kathryn J. Pflughoeft, David P. AuCoin.

Project administration: Derrick Hau, Sujata G. Pandit, Dana E. Reed, Marcellene A. Gates-Hollingsworth, Peter N. Thorkildson, Kathryn J. Pflughoeft, David P. AuCoin.

Resources: Derrick Hau, Marcellene A. Gates-Hollingsworth, Peter N. Thorkildson, David P. AuCoin.

Supervision: Derrick Hau, Sujata G. Pandit, Dana E. Reed, Haley L. DeMers, Teerapat Nualnoi, Marcellene A. Gates-Hollingsworth, Peter N. Thorkildson, Kathryn J. Pflughoeft, David P. AuCoin.

Validation: Derrick Hau, Brian Wade, Chris Lovejoy, Sujata G. Pandit, Haley L. DeMers, Heather R. Green, Emily E. Hannah, Megan E. McLarty, Cameron J. Creek, Chonnikarn Chokapirat, Jose Arias-Umana, Garrett F. Cecchini.

Visualization: Derrick Hau, Marcellene A. Gates-Hollingsworth, Peter N. Thorkildson, Kathryn J. Pflughoeft, David P. AuCoin.

Writing – original draft: Derrick Hau, Brian Wade, Marcellene A. Gates-Hollingsworth, Peter N. Thorkildson, Kathryn J. Pflughoeft, David P. AuCoin.

Writing – review & editing: Derrick Hau, Brian Wade, Chris Lovejoy, Sujata G. Pandit, Haley L. DeMers, Heather R. Green, Emily E. Hannah, Megan E. McLarty, Cameron J. Creek, Chonnikarn Chokapirat, Jose Arias-Umana, Garrett F. Cecchini, Teerapat Nualnoi, Marcellene A. Gates-Hollingsworth, Peter N. Thorkildson, Kathryn J. Pflughoeft, David P. AuCoin.

References

1. Benedictow O Jr. *The Black Death, 1346–1353: the complete history*. Woodbridge, Suffolk, UK; Rochester, N.Y., USA: Boydell Press; 2004. xvi, 433 pages p.
2. Stenseth NC, Atshabar BB, Begon M, Belmain SR, Bertherat E, Carniel E, et al. Plague: Past, Present, and Future. *PLoS Med*. 52008.
3. Lawrenz MB. Model Systems to Study Plague Pathogenesis and Develop New Therapeutics. *Front Microbiol*. 2010; 1. <https://doi.org/10.3389/fmicb.2010.00119> PMID: 21687720; PubMed Central PMCID: PMC3109633.
4. McCrumb FR Jr., Mercier S, Robic J, Bouillat M, Smadel JE, Woodward TE, et al. Chloramphenicol and terramycin in the treatment of pneumonic plague. *Am J Med*. 1953; 14(3):284–93. Epub 1953/03/01. [https://doi.org/10.1016/0002-9343\(53\)90040-0](https://doi.org/10.1016/0002-9343(53)90040-0) PMID: 13030486.
5. Butler T. Plague Gives Surprises in the First Decade of the 21st Century in the United States and Worldwide. *Am J Trop Med Hyg*. 2013; 89(4):788–93. <https://doi.org/10.4269/ajtmh.13-0191> PMID: 24043686; PubMed Central PMCID: PMC3795114.
6. Gage KL, Kosoy MY. Natural history of plague: perspectives from more than a century of research. *Annu Rev Entomol*. 2005; 50:505–28. Epub 2004/10/09. <https://doi.org/10.1146/annurev.ento.50.071803.130337> PMID: 15471529.
7. Plague around the world, 2010–2015. *Wkly Epidemiol Rec*. 2016; 91(8):89–93. PMID: 26922822.
8. Randlemanana R, Andrianaivoarimanana V, Nikolay B, Ramasindrazana B, Paireau J, Ten Bosch QA, et al. Epidemiological characteristics of an urban plague epidemic in Madagascar, August–November, 2017: an outbreak report. *Lancet Infect Dis*. 2019; 19(5):537–45. Epub 2019/04/02. [https://doi.org/10.1016/S1473-3099\(18\)30730-8](https://doi.org/10.1016/S1473-3099(18)30730-8) PMID: 30930106; PubMed Central PMCID: PMC6483974.
9. Riedel S. Plague: from natural disease to bioterrorism. *Proc (Bayl Univ Med Cent)*. 182005. p. 116–24. <https://doi.org/10.1080/08998280.2005.11928049> PMID: 16200159
10. Nguyen VK, Parra-Rojas C, Hernandez-Vargas EA. The 2017 plague outbreak in Madagascar: Data descriptions and epidemic modelling. *Epidemics*. 2018; 25:20–5. Epub 2018/06/06. <https://doi.org/10.1016/j.epidem.2018.05.001> PMID: 29866421.
11. Mead PS. Plague in Madagascar—A Tragic Opportunity for Improving Public Health. *N Engl J Med*. 2018; 378(2):106–8. Epub 2017/12/20. <https://doi.org/10.1056/NEJMp1713881> PMID: 29261403.
12. Majumder MS, Cohn EL, Santillana M, Brownstein JS. Estimation of Pneumonic Plague Transmission in Madagascar, August–November 2017. *PLoS Curr*. 10. <https://doi.org/10.1371/currents.outbreaks.1d0c9c5c01de69dfbff4316d772954f> PMID: 30450266; PubMed Central PMCID: PMC6224036.
13. Kool JL. Risk of person-to-person transmission of pneumonic plague. *Clin Infect Dis*. 2005; 40(8):1166–72. Epub 2005/03/26. <https://doi.org/10.1086/428617> PMID: 15791518.

14. Andrianaivoarimanana V, Wagner DM, Birdsell DN, Nikolay B, Rakotoarimanana F, Randriantseho LN, et al. Transmission of antimicrobial resistant *Yersinia pestis* during a pneumonic plague outbreak. *Clin Infect Dis*. 2021. Epub 20210709. <https://doi.org/10.1093/cid/ciab606> PMID: 34244722.
15. Spletstoesser WD, Rahalison L, Grunow R, Neubauer H, Chanteau S. Evaluation of a standardized F1 capsular antigen capture ELISA test kit for the rapid diagnosis of plague. *FEMS Immunol Med Microbiol*. 2004; 41(2):149–55. Epub 2004/05/18. <https://doi.org/10.1016/j.femsim.2004.02.005> PMID: 15145459.
16. Thullier P, Guglielmo V, Rajerison M, Chanteau S. Short report: Serodiagnosis of plague in humans and rats using a rapid test. *Am J Trop Med Hyg*. 2003; 69(4):450–1. Epub 2003/12/03. PMID: 14640508.
17. Tavares D, Bezerra M, Magalhães F, Cavalcanti T, Xavier C, Leal N, et al. A new recombinant F1 antigen as a cost and time-effective tool for plague diagnosis. *Journal of microbiological methods*. 2020; 172. <https://doi.org/10.1016/j.mimet.2020.105903> PMID: 32229265.
18. Tomaso H, Thullier P, Seibold E, Guglielmo V, Buckendahl A, Rahalison L, et al. Comparison of hand-held test kits, immunofluorescence microscopy, enzyme-linked immunosorbent assay, and flow cytometric analysis for rapid presumptive identification of *Yersinia pestis*. *J Clin Microbiol*. 2007; 45(10):3404–7. Epub 2007/07/27. <https://doi.org/10.1128/JCM.00458-07> PMID: 17652472; PubMed Central PMCID: PMC2045319.
19. Chanteau S, Rahalison L, Ralafiarisoa L, Foulon J, Ratsitorahina M, Ratsifasoamanana L, et al. Development and testing of a rapid diagnostic test for bubonic and pneumonic plague. *Lancet*. 2003; 361(9353):211–6. Epub 2003/01/28. [https://doi.org/10.1016/S0140-6736\(03\)12270-2](https://doi.org/10.1016/S0140-6736(03)12270-2) PMID: 12547544.
20. Rajerison M, Melocco M, Andrianaivoarimanana V, Rahajandraibe S, Rakotoarimanana F, Spiegel A, et al. Performance of plague rapid diagnostic test compared to bacteriology: a retrospective analysis of the data collected in Madagascar. *BMC infectious diseases*. 2020; 20(1). <https://doi.org/10.1186/s12879-020-4812-7> PMID: 32000692.
21. Jullien S, Dissanayake HA, Chaplin M. Rapid diagnostic tests for plague. The Cochrane database of systematic reviews. 2020; 6(6). <https://doi.org/10.1002/14651858.CD013459.pub2> PMID: 32597510.
22. Bertherat E, Thullier P, Shako JC, England K, Koné M-L, Arntzen L, et al. Lessons Learned about Pneumonic Plague Diagnosis from 2 Outbreaks, Democratic Republic of the Congo. *Emerging Infectious Diseases*. 2011; 17(5):778–84. <https://doi.org/10.3201/eid1705.100029> PMID: 21529384
23. Riehm JM, Rahalison L, Scholz HC, Thoma B, Pfeffer M, Razanakoto LM, et al. Detection of *Yersinia pestis* using real-time PCR in patients with suspected bubonic plague. *Mol Cell Probes*. 2011; 25(1):8–12. Epub 20101008. <https://doi.org/10.1016/j.mcp.2010.09.002> PMID: 20933595.
24. Winter CC, Cherry WB, Moody MD. An unusual strain of *Pasteurella pestis* isolated from a fatal human case of plague. *Bull World Health Organ*. 1960; 23(2–3):408–9. PMID: 13845309; PubMed Central PMCID: PMC2555592.
25. Sha J, Endsley JJ, Kirtley ML, Foltz SM, Huante MB, Erova TE, et al. Characterization of an F1 deletion mutant of *Yersinia pestis* CO92, pathogenic role of F1 antigen in bubonic and pneumonic plague, and evaluation of sensitivity and specificity of F1 antigen capture-based dipsticks. *J Clin Microbiol*. 2011; 49(5):1708–15. Epub 2011/03/04. <https://doi.org/10.1128/JCM.00064-11> PMID: 21367990; PubMed Central PMCID: PMC3122665.
26. Lukaszewski RA, Kenny DJ, Taylor R, Rees DG, Hartley MG, Oyston PC. Pathogenesis of *Yersinia pestis* infection in BALB/c mice: effects on host macrophages and neutrophils. *Infect Immun*. 2005; 73(11):7142–50. Epub 2005/10/22. <https://doi.org/10.1128/IAI.73.11.7142-7150.2005> PMID: 16239508; PubMed Central PMCID: PMC1273833.
27. Hu P, Elliott J, McCready P, Skowronski E, Garnes J, Kobayashi A, et al. Structural Organization of Virulence-Associated Plasmids of *Yersinia pestis*. *J Bacteriol*. 1998; 180(19):5192–202. <https://doi.org/10.1128/JB.180.19.5192-5202.1998> PMID: 9748454.
28. Prentice KW, DePalma L, Ramage JG, Sarwar J, Parameswaran N, Petersen J, et al. Comprehensive Laboratory Evaluation of a Lateral Flow Assay for the Detection of *Yersinia pestis*. *Health Secur*. 172019. p. 439–53. <https://doi.org/10.1089/hs.2019.0094> PMID: 31859568
29. Du Y, Rosqvist R, Forsberg A. Role of fraction 1 antigen of *Yersinia pestis* in inhibition of phagocytosis. *Infect Immun*. 2002; 70(3):1453–60. Epub 2002/02/21. <https://doi.org/10.1128/IAI.70.3.1453-1460.2002> PMID: 11854232; PubMed Central PMCID: PMC127752.
30. Chanteau S, Rahalison L, Ratsitorahina M, Mahafaly, Rasolomaharo M, Boisier P, et al. Early diagnosis of bubonic plague using F1 antigen capture ELISA assay and rapid immunogold dipstick. *Int J Med Microbiol*. 2000; 290(3):279–83. Epub 2000/08/26. [https://doi.org/10.1016/S1438-4221\(00\)80126-5](https://doi.org/10.1016/S1438-4221(00)80126-5) PMID: 10959730.
31. Williams JE, Gentry MK, Braden CA, Tyndal GL, Altieri PL, Berman S, et al. A monoclonal antibody for the specific diagnosis of plague. *Bull World Health Organ*. 1988; 66(1):77–82. Epub 1988/01/01. PMID: 3260145; PubMed Central PMCID: PMC2491117.

32. Lindler LE, Plano GV, Burland V, Mayhew GF, Blattner FR. Complete DNA Sequence and Detailed Analysis of the *Yersinia pestis* KIM5 Plasmid Encoding Murine Toxin and Capsular Antigen. *Infect Immun*. 1998; 66(19):5731–42. <https://doi.org/10.1128/IAI.66.12.5731-5742.1998> PMID: 9826348
33. Davis KJ, Fritz DL, Pitt ML, Welkos SL, Worsham PL, Friedlander AM. Pathology of experimental pneumonic plague produced by fraction 1-positive and fraction 1-negative *Yersinia pestis* in African green monkeys (*Cercopithecus aethiops*). *Arch Pathol Lab Med*. 1996; 120(2):156–63. Epub 1996/02/01. PMID: 8712895.
34. Mehigh RJ, Sample AK, Brubaker RR. Expression of the low calcium response in *Yersinia pestis*. *Microb Pathog*. 1989; 6(3):203–17. Epub 1989/03/01. [https://doi.org/10.1016/0882-4010\(89\)90070-3](https://doi.org/10.1016/0882-4010(89)90070-3) PMID: 2739560.
35. Reuter S, Connor TR, Barquist L, Walker D, Feltwell T, Harris SR, et al. Parallel independent evolution of pathogenicity within the genus *Yersinia*. *Proceedings of the National Academy of Sciences of the United States of America*. 2014; 111(18). <https://doi.org/10.1073/pnas.1317161111> PMID: 24753568.
36. Mueller CA, Broz P, Muller SA, Ringler P, Erne-Brand F, Sorg I, et al. The V-antigen of *Yersinia* forms a distinct structure at the tip of injectisome needles. *Science*. 2005; 310(5748):674–6. Epub 2005/10/29. <https://doi.org/10.1126/science.1118476> PMID: 16254184.
37. Pouliot K, Pan N, Wang S, Lu S, Lien E, Goguen JD. Evaluation of the role of LcrV-Toll-like receptor 2-mediated immunomodulation in the virulence of *Yersinia pestis*. *Infect Immun*. 2007; 75(7):3571–80. Epub 2007/04/18. <https://doi.org/10.1128/IAI.01644-06> PMID: 17438030; PubMed Central PMCID: PMC1932965.
38. Ligtenberg KG, Miller NC, Mitchell A, Plano GV, Schneewind O. LcrV mutants that abolish *Yersinia* type III injectisome function. *J Bacteriol*. 2013; 195(4):777–87. Epub 2012/12/12. <https://doi.org/10.1128/JB.02021-12> PMID: 23222719; PubMed Central PMCID: PMC3562105.
39. Perry RD, Harmon PA, Bowmer WS, Straley SC. A low-Ca²⁺ response operon encodes the V antigen of *Yersinia pestis*. *Infect Immun*. 1986; 54(2):428–34. <https://doi.org/10.1128/iai.54.2.428-434.1986> PMID: 3021629; PubMed Central PMCID: PMC260179.
40. Skrzypek E, Straley SC. Differential effects of deletions in lcrV on secretion of V antigen, regulation of the low-Ca²⁺ response, and virulence of *Yersinia pestis*. *J Bacteriol*. 1995; 177(9):2530–42. Epub 1995/05/01. <https://doi.org/10.1128/jb.177.9.2530-2542.1995> PMID: 7730287; PubMed Central PMCID: PMC176914.
41. Flashner Y, Fisher M, Tidhar A, Mechaly A, Gur D, Halperin G, et al. The search for early markers of plague: evidence for accumulation of soluble *Yersinia pestis* LcrV in bubonic and pneumonic mouse models of disease. *FEMS Immunol Med Microbiol*. 2010; 59(2):197–206. Epub 2010/05/26. <https://doi.org/10.1111/j.1574-695X.2010.00687.x> PMID: 20497221.
42. Gomes-Solecki MJC, Savitt AG, Rowehl R, Glass JD, Bliska JB, Dattwyler RJ. LcrV Capture Enzyme-Linked Immunosorbent Assay for Detection of *Yersinia pestis* from Human Samples. *Clin Diagn Lab Immunol*. 2005; 12(2):339–46. <https://doi.org/10.1128/CDLI.12.2.339-346.2005> PMID: 15699431
43. Ivashchenko TA, Belova EV, Dentovskaia SV, Bel'kova SA, Balakhonov SV, Ignatov SG, et al. [Development and testing of an enzyme immunoassay-based monoclonal test system for the detection of the *Yersinia pestis* V antigen]. *Prikl Biokhim Mikrobiol*. 2014; 50(2):211–8. Epub 2014/10/03. PMID: 25272741.
44. Rifflet A, Filali S, Chenau J, Simon S, Fenaille F, Junot C, et al. Quantification of low abundance *Yersinia pestis* markers in dried blood spots by immuno-capture and quantitative high-resolution targeted mass spectrometry. *Eur J Mass Spectrom (Chichester)*. 2019; 25(3):268–77. Epub 2019/05/18. <https://doi.org/10.1177/1469066718795978> PMID: 31096787.
45. Galimand M, Guiyoule A, Gerbaud G, Rasoamanana B, Chanteau S, Carniel E, et al. Multidrug resistance in *Yersinia pestis* mediated by a transferable plasmid. *N Engl J Med*. 1997; 337(10):677–80. Epub 1997/09/04. <https://doi.org/10.1056/NEJM199709043371004> PMID: 9278464.
46. Welch TJ, Fricke WF, McDermott PF, White DG, Rosso ML, Rasko DA, et al. Multiple antimicrobial resistance in plague: an emerging public health risk. *PLoS One*. 2007; 2(3):e309. Epub 2007/03/22. <https://doi.org/10.1371/journal.pone.0000309> PMID: 17375195; PubMed Central PMCID: PMC1819562.
47. Guiyoule A, Gerbaud G, Buchrieser C, Galimand M, Rahalison L, Chanteau S, et al. Transferable plasmid-mediated resistance to streptomycin in a clinical isolate of *Yersinia pestis*. *Emerg Infect Dis*. 2001; 7(1):43–8. <https://doi.org/10.3201/eid0701.010106> PMID: 11266293; PubMed Central PMCID: PMC2631670.
48. Kozel TR, Murphy WJ, Brandt S, Blazar BR, Lovchik JA, Thorkildson P, et al. mAbs to *Bacillus anthracis* capsular antigen for immunoprotection in anthrax and detection of antigenemia. *Proc Natl Acad Sci U S A*. 2004; 101(14):5042–7. Epub 2004/03/31. <https://doi.org/10.1073/pnas.0401351101> PMID: 15051894; PubMed Central PMCID: PMC387370.

49. Galyov EE, Smirnov OY, Karlishev AV, Volkovoy KI, Denesyuk AI, Nazimov IV, et al. Nucleotide sequence of the *Yersinia pestis* gene encoding F1 antigen and the primary structure of the protein. Putative T and B cell epitopes. *FEBS letters*. 1990; 277(1–2). [https://doi.org/10.1016/0014-5793\(90\)80852-a](https://doi.org/10.1016/0014-5793(90)80852-a) PMID: 1702734.
50. Vaidya HC, Beatty BG. Eliminating interference from heterophilic antibodies in a two-site immunoassay for creatine kinase MB by using F(ab')₂ conjugate and polyclonal mouse IgG. *Clin Chem*. 1992; 38(9):1737–42. Epub 1992/09/01. PMID: 1526006.
51. Cribbs DH, Ghochikyan A, Vasilevko V, Tran M, Petrushina I, Sadzikava N, et al. Adjuvant-dependent modulation of Th1 and Th2 responses to immunization with β -amyloid. *Int Immunol*. 2003; 15(4):505–14. <https://doi.org/10.1093/intimm/dxg049> PMID: 12663680; PubMed Central PMCID: PMC1483061.
52. Shibaki A, Katz SI. Induction of skewed Th1/Th2 T-cell differentiation via subcutaneous immunization with Freund's adjuvant. *Exp Dermatol*. 2002; 11(2):126–34. Epub 2002/05/08. <https://doi.org/10.1034/j.1600-0625.2002.110204.x> PMID: 11994139.
53. Nualnoi T, Kiro Singh A, Basallo K, Hau D, Gates-Hollingsworth MA, Thorkildson P, et al. Immunoglobulin G subclass switching impacts sensitivity of an immunoassay targeting *Francisella tularensis* lipopolysaccharide. *PLoS One*. 2018; 13(4):e0195308. Epub 2018/04/10. <https://doi.org/10.1371/journal.pone.0195308> PMID: 29630613; PubMed Central PMCID: PMC5890998.
54. Anisimov AP, Dentovskaya SV, Panfertsev EA, Svetoch TE, Kopylov PK, Segelke BW, et al. Amino acid and structural variability of *Yersinia pestis* LcrV protein. *Infect Genet Evol*. 2010; 10(1):137. <https://doi.org/10.1016/j.meegid.2009.10.003> PMID: 19835996; PubMed Central PMCID: PMC2818281.
55. Andrews GP, Heath DG, Anderson GW, Welkos SL, Friedlander AM. Fraction 1 capsular antigen (F1) purification from *Yersinia pestis* CO92 and from an *Escherichia coli* recombinant strain and efficacy against lethal plague challenge. *Infect Immun*. 1996; 64(6):2180–7. <https://doi.org/10.1128/iai.64.6.2180-2187.1996> PMID: 8675324; PubMed Central PMCID: PMC174053.
56. Wood WG. "Matrix effects" in immunoassays. *Scand J Clin Lab Invest Suppl*. 1991; 205:105–12. Epub 1991/01/01. PMID: 1947738.
57. Branger CG, Torres-Escobar A, Sun W, Perry R, Fetherston J, Roland KL, et al. Oral vaccination with LcrV from *Yersinia pestis* KIM delivered by live attenuated *Salmonella enterica* serovar Typhimurium elicits a protective immune response against challenge with *Yersinia pseudotuberculosis* and *Yersinia enterocolitica*. *Vaccine*. 2009; 27(39):5363–70. <https://doi.org/10.1016/j.vaccine.2009.06.078> PMID: 19596407
58. Zhou D, Tong Z, Song Y, Han Y, Pei D, Pang X, et al. Genetics of metabolic variations between *Yersinia pestis* biovars and the proposal of a new biovar, microtus. *J Bacteriol*. 2004; 186(15):5147–52. <https://doi.org/10.1128/JB.186.15.5147-5152.2004> PMID: 15262951; PubMed Central PMCID: PMC451627.
59. Revazishvili T, Rajanna C, Bakanidze L, Tsertsvadze N, Imnadze P, O'Connell K, et al. Characterisation of *Yersinia pestis* isolates from natural foci of plague in the Republic of Georgia, and their relationship to *Y. pestis* isolates from other countries. *Clinical microbiology and infection: the official publication of the European Society of Clinical Microbiology and Infectious Diseases*. 2008; 14(5). <https://doi.org/10.1111/j.1469-0691.2008.01953.x> PMID: 18294239.
60. Platonov ME, Evseeva VV, Dentovskaya SV, Anisimov AP. [Molecular typing of *Yersinia pestis*]. *Molekuliarnaia genetika, mikrobiologiya i virusologiya*. 2013;(2). PMID: 24003506.
61. Kopylov P, Platonov ME, Ablamunits VG, Kombarova TI, Ivanov SA, Kadnikova LA, et al. *Yersinia pestis* Caf1 Protein: Effect of Sequence Polymorphism on Intrinsic Disorder Propensity, Serological Cross-Reactivity and Cross-Protectivity of Isoforms. *PLoS One*. 2016; 11(9):e0162308. Epub 2016/09/09. <https://doi.org/10.1371/journal.pone.0162308> PMID: 27606595; PubMed Central PMCID: PMC5015843.
62. Une T, Brubaker RR. In vivo comparison of avirulent Vwa- and Pgm- or Pstr phenotypes of yersiniae. *Infect Immun*. 1984; 43(3):895–900. Epub 1984/03/01. <https://doi.org/10.1128/iai.43.3.895-900.1984> PMID: 6365786; PubMed Central PMCID: PMC264267.
63. Bearden SW, Fetherston JD, Perry RD. Genetic organization of the yersiniabactin biosynthetic region and construction of avirulent mutants in *Yersinia pestis*. *Infection and immunity*. 1997; 65(5). <https://doi.org/10.1128/iai.65.5.1659-1668.1997> PMID: 9125544.
64. DeMers HL, He S, Pandit SG, Hannah EE, Zhang Z, Yan F, et al. Development of an antigen detection assay for early point-of-care diagnosis of Zaire ebolavirus. *PLoS Negl Trop Dis*. 2020; 14(11):e0008817. Epub 2020/11/03. <https://doi.org/10.1371/journal.pntd.0008817> PMID: 33141837; PubMed Central PMCID: PMC7608863.
65. Hannah EE, Pandit SG, Hau D, Demers HL, Robichaux K, Nualnoi T, et al. Development of Immunoassays for Detection of *Francisella tularensis* Lipopolysaccharide in Tularemia Patient Samples. *Pathogens*. 2021; 10(8):924. <https://doi.org/10.3390/pathogens10080924> PMID: 34451388

66. Chanteau S, Rabarijaona L, O'Brien T, Rahalison L, Hager J, Boisier P, et al. F1 antigenaemia in bubonic plague patients, a marker of gravity and efficacy of therapy. *Trans R Soc Trop Med Hyg.* 1998; 92(5):572–3. Epub 1998/12/23. [https://doi.org/10.1016/s0035-9203\(98\)90923-3](https://doi.org/10.1016/s0035-9203(98)90923-3) PMID: 9861385.
67. Devadhasan JP, Gu J, Chen P, Smith S, Thomas B, Gates-Hollingsworth M, et al. Critical Comparison between Large and Mini Vertical Flow Immunoassay Platforms for. *Anal Chem.* 2021; 93(27):9337–44. Epub 20210514. <https://doi.org/10.1021/acs.analchem.0c05278> PMID: 33989499.
68. Riedel S. Biological warfare and bioterrorism: a historical review. *Proc (Bayl Univ Med Cent).* 172004. p. 400–6. <https://doi.org/10.1080/08998280.2004.11928002> PMID: 16200127
69. Wang X, Singh AK, Zhang X, Sun W. Induction of Protective Antiplague Immune Responses by Self-Adjuvanting Bionanoparticles Derived from Engineered *Yersinia pestis*. *Infection and immunity.* 2020; 88(5). <https://doi.org/10.1128/IAI.00081-20> PMID: 32152195.
70. Hamzabegovic F, Goll JB, Hooper WF, Frey S, Gelber CE, Abate G. Flagellin adjuvanted F1/V subunit plague vaccine induces T cell and functional antibody responses with unique gene signatures. *NPJ vaccines.* 2020; 5. <https://doi.org/10.1038/s41541-020-0156-y> PMID: 31993217.
71. Liu L, Wei D, Qu Z, Sun L, Miao Y, Yang Y, et al. A safety and immunogenicity study of a novel subunit plague vaccine in cynomolgus macaques. *Journal of applied toxicology: JAT.* 2018; 38(3). <https://doi.org/10.1002/jat.3550> PMID: 29134676.
72. Huang SS, Li IH, Hong PD, Yeh MK. Development of *Yersinia pestis* F1 antigen-loaded microspheres vaccine against plague. *International journal of nanomedicine.* 2014; 9. <https://doi.org/10.2147/IJN.S56260> PMID: 24550673.
73. Wang D, Jia N, Li P, Xing L, Wang X. Protection against lethal subcutaneous challenge of virulent *Y. pestis* strain 141 using an F1-V subunit vaccine. *Science in China Series C, Life sciences.* 2007; 50(5). <https://doi.org/10.1007/s11427-007-0071-8> PMID: 17879056.
74. Elvin SJ, Williamson ED. The F1 and V subunit vaccine protects against plague in the absence of IL-4 driven immune responses. *Microbial pathogenesis.* 2000; 29(4). <https://doi.org/10.1006/mpat.2000.0385> PMID: 10993741.
75. Daniel C, Sebbane F, Poiret S, Goudercourt D, Dewulf J, Mullet C, et al. Protection against *Yersinia pseudotuberculosis* infection conferred by a *Lactococcus lactis* mucosal delivery vector secreting LcrV. *Vaccine.* 2009; 27(8):1141–4. Epub 20090109. <https://doi.org/10.1016/j.vaccine.2008.12.022> PMID: 19135495.
76. Nelson CA, Meaney-Delman D, Fleck-Derderian S, Cooley KM, Yu PA, Mead PS, et al. Antimicrobial Treatment and Prophylaxis of Plague: Recommendations for Naturally Acquired Infections and Bioterrorism Response. *MMWR Recomm Rep.* 2021; 70(3):1–27. Epub 20210716. <https://doi.org/10.15585/mmwr.rr7003a1> PMID: 34264565; PubMed Central PMCID: PMC8312557.
77. Thomas CU, Hughes PE. Plague Surveillance by Serological Testing of Coyotes (*Canis latrans*) in Los Angeles County, California. *Journal of Wildlife Diseases.* 1992; 28(4):610–3. <https://doi.org/10.7589/0090-3558-28.4.610> PMID: 1474660
78. Abbott RC, Hudak R, Mondesire R, Baeten LA, Russell RE, Rocke TE. A rapid field test for sylvatic plague exposure in wild animals. *J Wildl Dis.* 2014; 50(2):384–8. Epub 2014/02/04. <https://doi.org/10.7589/2013-07-174> PMID: 24484483.
79. Philipovskiy AV, Cowan C, Wulff-Strobel CR, Burnett SH, Kerschen EJ, Cohen DA, et al. Antibody against V Antigen Prevents Yop-Dependent Growth of *Yersinia pestis*. *Infect Immun.* 732005. p. 1532–42. <https://doi.org/10.1128/IAI.73.3.1532-1542.2005> PMID: 15731051
80. Anderson GW Jr., Worsham PL, Bolt CR, Andrews GP, Welkos SL, Friedlander AM, et al. Protection of mice from fatal bubonic and pneumonic plague by passive immunization with monoclonal antibodies against the F1 protein of *Yersinia pestis*. *Am J Trop Med Hyg.* 1997; 56(4):471–3. Epub 1997/04/01. <https://doi.org/10.4269/ajtmh.1997.56.471> PMID: 9158060.
81. Xiao X, Zhu Z, Dankmeyer JL, Wormald MM, Fast RL, Worsham PL, et al. Human Anti-Plague Monoclonal Antibodies Protect Mice from *Yersinia pestis* in a Bubonic Plague Model. *PLoS One.* 52010.
82. Hill J, Copse C, Leary S, Stagg AJ, Williamson ED, Titball RW. Synergistic Protection of Mice against Plague with Monoclonal Antibodies Specific for the F1 and V Antigens of *Yersinia pestis*. *Infect Immun.* 712003. p. 2234–8. <https://doi.org/10.1128/IAI.71.4.2234-2238.2003> PMID: 12654847
83. Broz P, Mueller CA, Muller SA, Philippsen A, Sorg I, Engel A, et al. Function and molecular architecture of the *Yersinia* injectisome tip complex. *Mol Microbiol.* 2007; 65(5):1311–20. Epub 2007/08/19. <https://doi.org/10.1111/j.1365-2958.2007.05871.x> PMID: 17697254.
84. Wang S, Heilman D, Liu F, Giehl T, Joshi S, Huang X, et al. A DNA vaccine producing LcrV antigen in oligomers is effective in protecting mice from lethal mucosal challenge of plague. *Vaccine.* 222004. p. 3348–57. <https://doi.org/10.1016/j.vaccine.2004.02.036> PMID: 15308359